C.P. No. 1142

C.P. No. 1142

MINISTRY OF AVIATION SUPPLY

AERONAUTICAL RESEARCH COUNCIL

CURRENT PAPERS

A Novel Method for the Estimation of the Zero-Lift Forebody Pressure Drag of Axisymmetric Non-Slender Shapes at Supersonic and Hypersonic Velocities

By

P. G. Pugh and L. C. Ward

Aerodynamics Division, NPL

LONDON HER MAJESTY'S STATIONERY OFFICE

1971

Price 40p net

C.P. No. 1142*
February 1970

A Novel Method for the Estimation of the Zero-Lift Forebody Pressure Drag of Axisymmetric Non-Slender Shapes at Supersonic and Hypersonic Velocities

- By -
P. G. Pugh and L. C. Ward
Aerodynamics Divn., NPL

SUMMARY

The method described in this paper uses the novel approach of first predicting the shape of the bow shock wave and then using this to calculate the drag through a computation of the total rate of entropy production due to the bow shock wave. Both blunted and sharp forebodies can be treated in this way and comparison with experimental data shows that drag predictions with a typical accuracy of 5% are readily achieved. The method has been expressly developed to be economical in its use of computer time so as to allow of its repetitive use in optimisation studies.

1✓

---

* Replaces NPL Aero Special Report 038 - A.R.C.31 761

1. Introduction

Recent studies have shown, that for most constraints of practical importance, the optimum forebody shape for a supersonic vehicle will feature a considerable degree of nose rounding. Existing simple theoretical methods for calculating forebody drag are inadequate since such shapes are outside their range of validity. Optimisation studies are thus often restricted to the time consuming and uncertain process of interpolation using available experimental data. Thus, there is an urgent need for a method of forebody drag estimation which is sufficiently accurate to enable promising forebody shapes to be readily identified, and yet is sufficiently simple to allow of its repetitive use in optimisation studies without undue cost in computing time. Since it will be required to cope with a wide range of forebody configurations, it is important that such a method makes as little use as possible of empirical correlations whose validity is necessarily confined to the range of experimental data used in their compilation.

Most simple methods of pressure drag estimation proceed through the prediction of pressure distributions which, when integrated, yield the pressure drag. This has proved to be a difficult task in the case of round nosed bodies unless extensive empirical data are employed. The major difficulty lies in the treatment of regions of high surface curvature and their downstream influence.

However, following the successful development of methods for the estimation of forebody pressure drag from measured bow shock-wave shapes,[2] attention has been given to the possibility of predicting the shock wave shape for a given body, and hence estimating its drag. This approach has met with some success. The purpose of this note is to outline the essential features of this scheme as this approach may be of help to other workers in the field of drag estimation. While the method is still capable of refinement and extension, sufficient success has been achieved to justify making the basic approach more generally available.

In the following description of the method, attention is concentrated on the simplest practical forebody shape which incorporates nose rounding, namely the spherically blunted cone. This shape was chosen because of its simplicity and because sufficient reliable experimental drag data exist to enable the success of the proposed prediction method to be judged. However, as indicated in the following section, the prediction method is capable of dealing with a wide range of other forebody shapes.

In assessing the success of this method it must be appreciated that it is unlikely that any simple method will ever be developed which will allow of the very accurate estimation of absolute levels of drag for non-slender shapes. However, although one of the aims of the present method is to predict absolute levels of drag with reasonable precision, the primary purpose is to predict reliable trends in the variation of drag coefficient with body geometry, in order to enable optimum shapes to be identified reasonably accurately and thus minimise the inevitable 'cut-and-try' wind tunnel tests.

2. The basic scheme

As indicated above, the method adopted is to predict the shape of the bow shock wave for a given body and hence use the existing calculation procedures to estimate the forebody drag. The problem of predicting the forebody drag has been simplified by dividing the bow shock wave into various zones. For example, in the case of the blunted cone, it is sufficient to consider three zones which may be defined by considering the regions of influence of the various parts of the

/body

body (see Fig. 1). These are:-

I, the shock-wave shape due to the blunting

II, a near-conical portion of the shock wave

III, the decay of the bow shock wave to a Mach wave.

Zone I arises from the embedded subsonic flow close to the axis of symmetry and the interaction between the bow shock wave and the expansion from the sonic point to the bluntness/cone junction. The influence of the bluntness on the shock wave terminates when the bow shock wave is intersected by the most downstream characteristic to spring from the bluntness/cone junction.

Zone II arises from the flow over the conical portion of the body and lies between the end of Zone I and the point at which the most upstream characteristic of the expansion fan radiating from the discontinuity of slope at the base of the cone intersects the shock wave.

Zone III is determined by the interaction of the expansion from the base of the cone and the bow shock wave. This zone stretches from the end of Zone II to infinity.

The prediction method used is a marching solution predicting the shape and location of Zones I, II, and III in that order and using each prediction to provide boundary conditions for the next stage of the calculation.

Accordingly, the methods used for each section will be described in turn, followed by a description of the methods used to match each solution to form the whole shock wave.

More complex body geometries are dealt with by approximating the body shape by a "blunting" followed by a series of cone frustrums. The complete bow shock wave due to the blunting and the first cone frustrum is then calculated. This blunted cone is then treated as the "bluntness" applied to the second cone frustrum and the previously calculated shock shape is used as an input to this second calculation. This cycle is repeated until the bow shock wave due to the complete body has been calculated. Because of the simplicity of the calculation method adopted, computing time for each cycle is extremely short (approx. 8 secs machine running time on an I.C.L. KDF-9). Thus a large number of cone frustrums may be used to approximate the shape of a smooth body to a high degree of accuracy.

2.1 Zone I - The part of the shock due to the blunting

The shape of this part of the bow shock wave is determined by the geometrical shape of the bluntness alone and scales linearly as the bluntness size. The prediction method uses experimentally measured shock-wave shapes for isolated bodies which are geometrically similar to that part of the nose blunting that is wetted by the flow. Thus, measured shock wave shapes for isolated spheres are used in the calculation of bow shock waves due to spherically blunted cones while measured shock-wave shapes for isolated discs are used in the treatment of flat-faced truncated cones. The acceptance of this empirical input avoids the exceedingly arduous task of computing the mixed subsonic/transonic flow around the bluntness. It does not, however, unduly restrict the range of the whole prediction method. For example, a single measured shock-wave shape for an isolated sphere at a given Mach number is all that is required to predict the drag of any spherically blunted configuration at that Mach number. Indeed, such a

/measured

measured shock-wave shape for an isolated sphere is sufficient for the prediction of the drag of any body in which the blunting takes the form of a segment of a sphere whether or not there is a discontinuity of slope at the bluntness/cone junction. However, all the examples presented in this paper are for spherically blunted cones in which the distribution of surface slope is continuous (i.e. there is no change in slope at the sphere/cone junction). The measured shock-wave shapes must be accurate - to the same standard as required for their use to estimate forebody drag[2,7] - and to extend to values of y/D such that the shock angle closely approaches a Mach wave. However, in fitting a "standard" bluntness shape to the stagnation region of an arbitary forebody geometry some degree of approximation is probably acceptable. Inverse numerical calculations of the embedded subsonic flow due to a prescribed shock wave have shown that extremely small differences in shock-wave shape produce widely different body geometries in the vicinity of the stagnation point. Thus some discrepancies in the fitting of the given body shape by a "standard bluntness" in the stagnation region is probably reasonable provided that the fit is good in the vicinity of the sonic point - which can readily be established by standard methods.

In the computational scheme adopted this shock-wave shape is specified by a table of pairs of co-ordinates of points on the shock wave due to an "isolated bluntness" of unit maximum diameter together with shock slopes at these points.

The prediction of this portion of the shock wave thus reduces to simply taking each pair of co-ordinates and scaling these by the factor required to scale the "isolated bluntness" so that it is identical with the actual blunting over the wetted area of the latter.

2.2 Zone II - Quasi-conical shock wave

It is commonly observed that for blunted cones the zone of the bow shock wave lying immediately downstream of the end of the highly curved section (Zone I) is virtually conical. Several workers, noteably Traugott[11], have commented upon the appearence of points of inflection in bow shock waves due to blunted bodies. These are significant only under rather extreme conditions such as large cone angles for which the Mach number of the flow over the surface of the cone is near unity, and, in general, are important only when internal shock waves are present between the bow shock wave and the body. During the course of measurements of observed bow shock waves about a wide range of blunted cones, it was found to be difficult to distinguish a point of inflection despite the fact that the measurement accuracy was amply sufficient to enable satisfactory estimates of overall forebody pressure drag to be made. It is, therefore, considered unnecessary to allow for deviations of the bow shock wave in Zone II from a conical form provided that the mean shock angle is correctly predicted.

However, it must be noted that the true mean shock angle is not that which corresponds to a sharp cone of the same semi-apex angle as the conical portion of the body. This discrepancy arises from the presence of an entropy layer enveloping the surface of the cone. This layer comprises the gas which has passed through the strong shock wave near the axis of symmetry and has suffered a large increase in entropy. It is commonly observed that the surface pressure on the conical portion of blunted cones attains an approximately constant value a short distance downstream of the bluntness/cone junction (i.e. although important "overexpansions" occur, the large percentage deviations from a uniform pressure are confined to a small region near the junction). Thus, the greater entropy of the gas near the cone surface implies that the gas density is correspondingly low. Accordingly, by analogy with a boundary layer, this entropy layer may be regarded as having a displacement effect. Unlike the boundary layer, the displacement area of the entropy layer is constant over most of the surface of the conical part of the body because high shock angles are confined to a region of the shock wave close to the axis of symmetry. As the entropy layer develops downstream it is spread around an

/increasing

increasing cone periphery. This means that the displacement thickness decreases in the downstream direction, making the mean inclination of the displacement surface less than that of the solid surface of the conical part of the body.

The excess of entropy in the entropy layer over that of the rest of the flow between the bow shock wave and the body arises because the shock angles in Zone I are greater than they would have been if the body had been sharp. Thus, the excess entropy is due to the shape of the shock wave in Zone I. Since the change in shock angle due to the presence of the entropy layer, although of significance in calculating the overall drag, is small, it is justifiable to make approximations in the calculation of the displacement area.

A simple relationship may be developed along the lines indicated below:-

Consider a blunted cylinder. In this case the entropy layer arises as a result of the whole shock wave because the bow shock wave due to the parallel portion of the body is the limiting case of a Mach wave. Thus, we can write for each streamline, considering conditions in the streamline and at a point downstream of the bow shock wave:-

$$\Delta S = c_p.\log_e(T_d/T_\infty) + R.\log_e(p_\infty/p_d).$$

If the downstream point is far downstream of the nose, $p_d = p_\infty$. Also, if the free stream Mach number is not too high, then $\frac{\Delta S}{\gamma c_v} \ll 1$ everywhere. Thus, using the series expansion for $\log_e$ and the binomial theorem:-

$$\frac{T_d}{T_\infty} \simeq 1 + \frac{\Delta S}{\gamma c_v} \qquad \ldots(1)$$

and since $p_d = p_\infty$ we have $\rho_d T_d = \rho_\infty T_\infty$

and hence

$$\frac{\rho_d}{\rho_\infty} \simeq 1 - \frac{\Delta S}{\gamma c_v}. \qquad \ldots(2)$$

To obtain the downstream velocity we use the energy equation

$$\frac{u_\infty^2}{2} + \frac{a_\infty^2}{(\gamma-1)} = \frac{u_d^2}{2} + \frac{a_d^2}{(\gamma-1)}\ ; \qquad \ldots(3)$$

and since

$$\frac{a_\infty}{a_d} = \left(\frac{T_\infty}{T_d}\right)^{\frac{1}{2}},$$

$$\frac{a_d^2}{a_\infty^2} = \frac{T_d}{T_\infty} \approx 1 + \frac{\Delta S}{\gamma c_v} \quad \text{(from (1))}.$$

Then substituting in (3), we obtain

$$\frac{u_d}{u_\infty} \simeq 1 - \frac{1}{(\gamma-1)M_\infty^2} \cdot \frac{\Delta S}{\gamma c_v} . \qquad \ldots(4)$$

Now the effective displacement area produced by the entropy layer is

$$\delta = \int_0^\infty \left(1 - \frac{\rho_d u_d}{\rho_\infty u_\infty} \right) \cdot 2\pi y dy \qquad \ldots(5)$$

and from (2) and (4) we obtain

$$\frac{\rho_d u_d}{\rho_\infty u_\infty} = 1 - \frac{\Delta S}{\gamma c_v} \left\{ 1 + \frac{1}{(\gamma-1)M_\infty^2} \right\}$$

$$= 1 - Z \frac{\Delta S}{c_v}, \quad \text{say}$$

$$\text{where} \qquad Z = \frac{1}{\gamma} \left\{ 1 + \frac{1}{(\gamma-1)M_\infty^2} \right\} . \qquad \ldots(6)$$

Hence $$\delta = 2 \int_0^\infty Z \frac{\Delta S}{c_v} \pi y \, dy.$$

This can be related to K, the forebody drag, by means of Oswatitsch's theorem (Ref.1, p.209) which gives (to first order in ΔS)

$$K = 2\rho_\infty T_\infty \int_0^\infty \Delta S \pi y \, dy. \qquad \ldots(7)$$

Hence

$$\delta = \frac{ZD}{c_v \rho_\infty T_\infty} = \frac{1}{2} Z.A.C_D.\gamma(\gamma-1).M_\infty^2 \qquad \ldots(8)$$

$$\text{so} \quad \eta = \frac{\text{Displacement Area}}{\text{Max. cross-sectional area of body}} = \frac{1}{2} C_D \left\{ 1 + (\gamma-1).M_\infty^2 \right\}. \qquad \ldots(9)$$

Thus the total displacement thickness is directly related to the forebody pressure drag of the blunting (in this case the complete body). It should be noted that equation (9) does not involve the geometry of the body in any way except through C_D.

Turning now to the case where the part of the body downstream of the blunting has a non-zero inclination to the free-stream (and hence a non-zero pressure drag), two additional factors have to be taken into account. Firstly, the entire flow between the body and the bow shock wave suffers some increase in entropy even if the blunting is vanishingly small. The entropy layer then results from the excess of entropy near the body compared to the entropy of the majority of flow within the shock layer. Neglecting second order effects (such as the fact that the presence of the entropy layer alters the strength of the conical portion of the shock wave and hence reacts back on the entropy layer thickness), the whole of the excess entropy production is confined to Zone I of the shock wave, and results from the replacement of part of the conical shock wave due to a sharp nosed cone by the curved shock due to the blunting. Recalling the proportionality between drag and rate of entropy production, it is reasonable, therefore, to allow for this effect by replacing C_D in equation (9) by the difference in drag coefficients between that of the "isolated bluntness" and the section of the conical body replaced by the bluntness. Further, the pressure on the surface of the conical portion of the body is higher than free-stream pressure. Since the Mach numbers, including those within the entropy layer, are considerably in excess of unity, the mass flux densities close to the surface are increased because the Mach number is lower than it would have been had the surface been aligned with the free-stream direction. If the mass flux densities over the inclined and cylindrical surfaces are related by the isentropic relation to sufficient accuracy (which will be the case unless the inclined surface is at a large angle to the free-stream direction) and if the Mach numbers in the entropy layer are not too close to unity then we may write:-

$$G = \frac{\text{Displacement area on inclined surface}}{\text{Displacement area on cylindrical surface}} \approx ((\gamma . M_\infty^2 . C_p)/2 + 1)^{-1/\gamma} \quad \ldots\ldots (10)$$

This approximation implies that the main cause of the variation of mass flux per unit area is the change in density. This is physically reasonable for supersonic Mach numbers not too close to unity when the kinetic energy of the gas is considerably larger than its internal energy so that small changes in velocity are accompanied by large changes in density.

To the same degree of approximation as used earlier we may write

$C_p = C_{p_s}$ where C_{p_s} is the pressure coefficient over the forward facing surfaces of a sharp cone of the same apex angle as the conical portion of the body. That is to say, it is considered necessary to allow for the effects of the entropy layer on shock angle, but that this effect is sufficiently small to allow the use of approximate methods in its calculation without incurring significant errors in the computation of the overall drag of the body. Thus, in calculating the entropy layer thickness (but not the total drag) it may be assumed that the angle of the conical part of the shock wave is the same as that due to a sharp cone of the same apex angle as the conical portion of the body. This is no more than to say that if the fractional change of total drag due to the presence of the entropy layer is δ then δ is significant compared to 1 but that δ^2 may be neglected - a not unreasonable assumption for most cases.

Thus the effective cone angle (i.e. the inclination of the displacement surface to the free-stream) is calculated from the geometry of the conical part of the body and the displacement area of the entropy layer computed as described above - which, as discussed earlier, is assumed to be constant. The shock wave

/inclination

inclination in Zone II is then computed using the exact numerical solutions of Simms[3] and the interpolation tables of Crabbe and Cambell[4].

2.3 Zone III - Decaying axi-symmetric shock wave

The interaction of the bow shock wave with the expansion fan could be calculated exactly by the method of characteristics provided the flow conditions on the most upstream characteristic were known. This would be a time consuming process and hence it would be undesirable to include a characteristics calculation into the present method especially since it would have to be a complex non-homentropic calculation including shock waves. Again, it is doubtful whether, with reasonable effort, the requisite boundary conditions could be specified with sufficient accuracy to merit this approach. The prime difficulty that has to be overcome in developing a simpler approach is the variation in flow properties between the shock and the body. This variation is due to two causes.

Firstly, the presence of the entropy layer introduces significant gradients in the flow properties close to the body surface. However, at the base the entropy layer is spread out over a large periphery and hence its effects are generally confined to distances from the body which are small compared to the distance between the shock and the body (measured along the most upstream characteristic of the expansion). The entropy layer would thus be expected to cause only a small displacement of the outgoing characteristics from the positions that they would have taken up in the absence of the entropy layer.

The second cause of variations in flow properties between the body and the shock wave is that, even if the body were a sharp cone, flow property variations of this type would occur because of the axisymmetric nature of the flow. Thus the outgoing characteristics are curved and the degree of curvature depends on the relative magnitudes of the flow deflections at the shock and at the body. Since the present objective is to predict the shock-wave shape and not the whole flow field the parameter of importance is the mean inclination of the characteristic (ϕ say)* and its relationship to β (the shock angle to the free-stream at the point where the characteristic intersects the shock wave). If a unique relationship between ϕ and β could be established for a given free-stream Mach number then a simple solution for the shape of the shock in Zone III is possible. Such a simple solution would, of course, apply only to the general class of flow situations being considered, i.e. the interaction of an axisymmetric shock wave and an expansion, and not to all flow fields.

In the analogous two-dimensional case such a relation is known to exist since, to a high degree of approximation, the shock wave bisects the angle between the characteristics upstream and downstream of the shock wave.

i.e. $(\mu + \phi)/2 = \beta$ ..... (11)

or $\mu + \phi = 2\beta$

hence $\phi = 2\beta - \mu$ ..... (12)

The same relationship must apply to all flows if ϕ is replaced by ϕ_s where ϕ_s is the inclination of the characteristic immediately downstream of the shock wave.

/Similar

---

* In this context the "mean inclination" of the characteristic is the angle between the free stream and the straight line joining the points at which the characteristic intersects the body and at which it intersects the shock wave.

Similar relations such as:-

$$\phi - \mu = f(\beta - \mu) \quad \text{or:} \quad \phi \cdot f(\beta) \qquad \ldots\ldots (13)$$

might also be expected for axi-symmetric flow. While it is not proposed to demonstrate this from first principles, there is strong circumstantial evidence to support this suggestion. For example, this suggestion can be tested experimentally wherever the expansion fan is centred on a discontinuity of surface slope. Then the origin of the characteristics is known (i.e. at the discontinuity) so that the mean inclination of any characteristic intersecting a point on the shock wave may be readily estimated from a measured shock-wave shape. This has been done for a disc, two cut spheres, and a 40° half angle cone, the results being shown in Fig. (2a).

In this figure these experimental results are compared with exact numerical solutions which were obtained using a computer program due to Moore[5]. The numerical results give the β, ϕ relationship for the most upstream characteristic of the expansion fan (for a wide range of sharp cones).

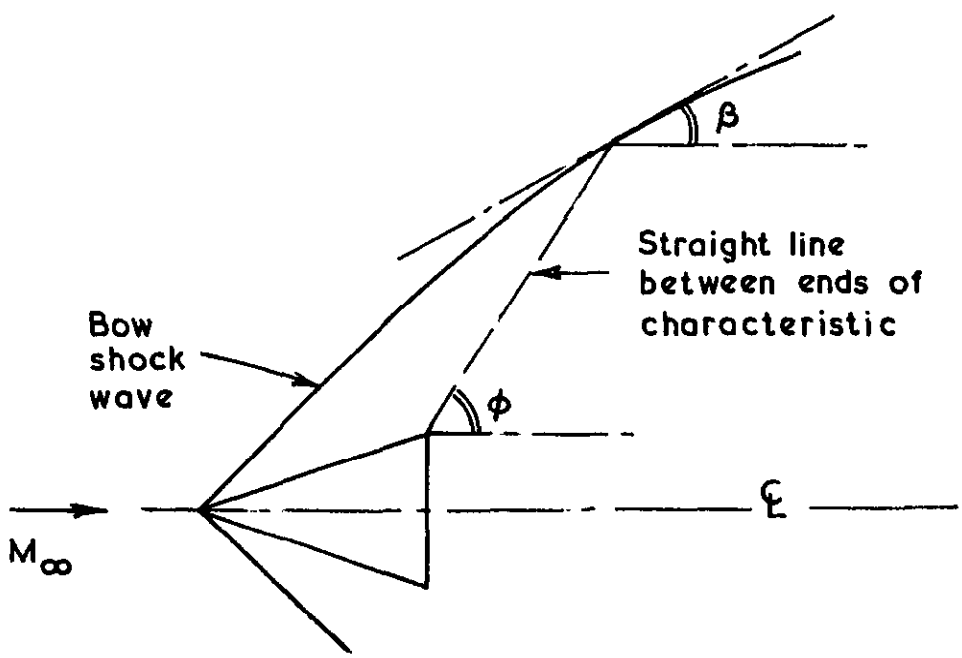

SKETCH 1

The experimental results demonstrate the similarity between the decaying bow shock waves about several different body geometries. They also suggest that there is, at least to a reasonable approximation, a unique relationship between β and ϕ for each free-stream Mach number. There is a significant difference between the experimental results and the numerical solutions at values of shock angle (β) greater than about 30°.

/Since

Since the experimental results for shock angles greater than 30° correspond to characteristics deep inside the expansion fan, whereas the numerical results are all for the most upstream characteristic of the expansion, Fig. (2a) is interpreted as showing that there is some effect of the position of a characteristic within an expansion on its mean inclination to the free-stream direction. This effect is, however, remarkably small considering that the strength of the expansion preceeding a characteristic in question varies so widely between the different results shown on Fig. (2a). This suggests that it might well be adequate to assume a unique relationship between β and ϕ for any given Mach number and yet preserve useful accuracy in the prediction of the shape of the bow shock wave in zone III.

It is also interesting to examine the possibility of using a relationship of the form $(\phi-\mu)=f(\beta-\mu)$ to cover a range of free-stream Mach numbers. In Fig. 2b, plots of $(\phi-\mu)$ and $(\beta-\mu)$ are given for the most upstream characteristic of the expansion fan for a wide range of sharp cones at two very different Mach numbers. Also shown is the relationship $\phi=2\beta-\mu$ (for two dimensional flow) referred to earlier.

There is an interesting degree of correlation between the curves shown in Fig. 2b. However, it is clear that the use of a unique relationship of the form $(\phi-\mu)=f(\beta-\mu)$ to cover all Mach numbers would introduce additional significant errors. Accordingly, pending the development of a more general expression, the current prediction method uses a different relationship between $(\phi-\mu)$ and $(\beta-\mu)$ for each free-stream Mach number considered.

The relationship chosen was that given by the theory. This was adopted for the following reasons:-

a) it could be readily and precisely calculated for any chosen free-stream Mach number.

b) Analysis of measured shock-wave shapes has shown that good estimates of forebody pressure drag can be obtained from the shock-wave shape[2] only if the shape of the shock wave at large distances from the body is reasonably well defined or predicted and if the shape of the bow shock wave is known precisely in the vicinity of the junction between Zones II and III. Since the numerical results apply to the case of zero strength for the expansion upstream of the characteristic considered, the β, ϕ relationship derived from them is more likely to be correct in the vicinity of the junction between Zones II and III. Further, the same β, ϕ relationship seems in good agreement with the experimental results for shock angles close to the Mach angle.

c) Complex body geometries are built up from a multiplicity of cone frustrums when applying the method described in this paper. In this case zones like Zone II and Zone III alternate and the expansion fans between each conical segment of the shock wave become weak. In this case the numerical calculations are likely to represent the truth more closely for the reasons outlined above.

For simplicity the chosen β, ϕ relationship was approximated by two straight lines, the maximum deviation of the calculated points from this approximation giving 0.02° error in the value of β corresponding to a given value of ϕ.

If such a relationship between β and ϕ is adopted, then calculation of Zone III merely becomes an exercise in geometry, the solution proceeding in a marching fashion downstream from the initial conditions given by the shock angle in Zone II, and the geometry of the base plane of the model.

/This

This calculation procedure should, strictly speaking, be continued to infinity in the y and x directions if subsequent integration of the rate of entropy production at the bow shock wave is to yield the total forebody pressure drag. To avoid thus attempting the impossible, the marching solution is terminated at $(\beta-\mu)\approx 0.006°$ corresponding to a value of (y/D) which always exceeds 200. At this distance from the body, the flow behind the bow shock wave will have taken on the familiar far-field form having an N-wave pressure trace. Accordingly, the analysis due to Luidens[12] is applicable. This gives the result that:-

$$\frac{K_e}{K} = 1 - \left(\frac{L}{l}\right) \qquad \text{.....(14)}$$

(equation 27 of Ref. 12)

where K_e is the drag due to entropy production at all points on the shock wave between $0 \leq (y/D) \leq (y/D)'$, $(y/D)'$ being the value of (y/D) at which the marching solution is terminated. The term l is the distance, measured in the free-stream direction, from the last point on the bow shock wave calculated by the marching solution, to a line drawn from the origin of the last expansion at angle μ to the free stream.

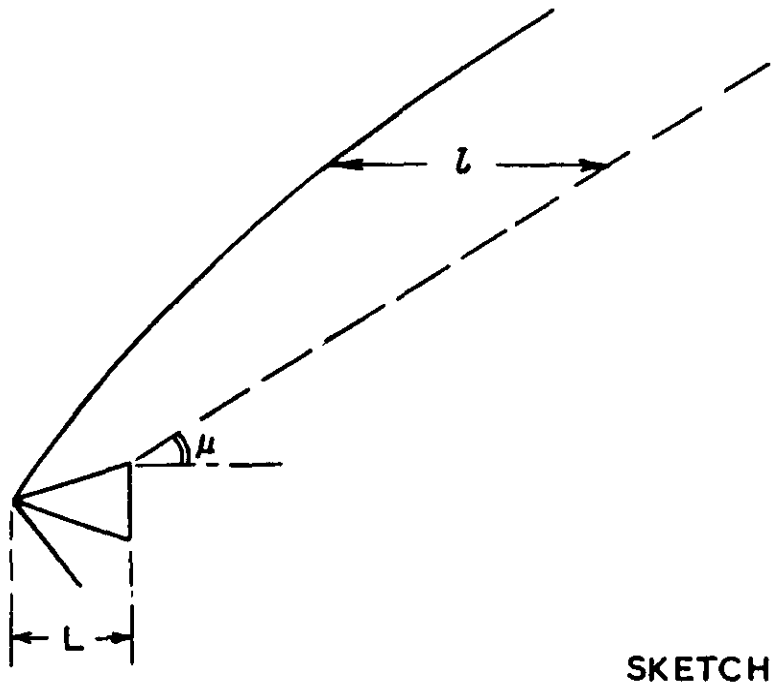

SKETCH 2

Thus, the calculated shock shape for $(y/D) \leq (y/D)'$ may be used together with equation (14) to evaluate the total forebody pressure drag without having to extend the marching solution (used to calculate the shock shape in Zone III for $(y/D) < (y/D)'$) to extreme values of (y/D). The total computing time is thus kept at an acceptable level at the same time as reasonable accuracy is retained.

3. Matching procedures

It remains to match the solutions for Zones I, II and III so as to produce a complete predicted bow shock-wave shape.

/This

This problem is one of predicting the location of various "junction" characteristics. For example, since Zone I is determined by the shape of the bluntness and Zone II is likewise determined by the shape of the displacement surface over the conical portion of the body, Zones I and II join at the point where the outgoing characteristic from the bluntness/cone junction intersects the bow shock wave. If strong internal shock waves are present the problem is more complex and cannot be treated at present. However, if the flow between the bow shock wave and the body is isentropic (or effectively so) then the matching point between Zones I and II may be found either by:-

a) finding the point at which the calculation of Zone I yields a shock wave angle equal to that of the shock wave in Zone II,

or b) calculating the mean inclination of the junction characteristic from the shock angle in Zone II and hence finding the point at which this characteristic meets the bow shock wave as calculated using the method appropriate to Zone I.

However, for most configurations of practical importance matching takes place at values of β such that the experimental β, ϕ relationship for blunt configurations is not much different to that computed for conical flow fields. Thus, the matching points calculated by both methods will be in good agreement. Either method should give satisfactory results and, for computational convenience, the former is currently used.

Since the shock slope at this matching point depends on the displacement area of the entropy layer and this, in turn, varies as the shock slope, some iteration is required in principle. However, as noted in section 2b, this coupling is a second order effect, and in practice, such iteration is not required.

The matching procedure for Zones II and III is implicit in the beginning of the marching solution for Zone III. Since a given relationship between β and ϕ is assumed, this applies to all outgoing characteristics of the expansion centred on the periphery of the base of the model. Thus a knowledge of the shock angle within Zone II enables the mean inclination of the most upstream characteristic of the expansion to be calculated. The shock-wave shape within Zone II is known and the origin and slope of this most upstream characteristic of the expansion can then be derived. Thus their intersection (the junction of the two zones) may readily be calculated.

4. Complete calculation scheme

The foregoing principles for the prediction of forebody pressure drag have been realised in a computer program, which performs the following major steps:-

1) Reads in the shock-wave shape about the "isolated bluntness" from a data tape.
2) Scales these data to the actual bluntness size.
3) Calculates the displacement area of the entropy layer and hence the mean inclination of the displacement surface over the conical part of the body.
4) Calculates the shock angle in Zone II.
5) Determines the matching point between Zones I and II and hence the shock shape in these two Zones.
6) Determines the matching point for Zones II and III.
7) Computes the shock shape in Zone III.
8) Calculates the forebody pressure drag from the bow shock-wave shape as in Ref (2).
9) Allows for entropy production at points on the shock wave for $(y/D) > (y/D)'$ (Equ. 14).

/if

If a curved forebody has been approximated by several segments, then steps 1) to 8) are carried out for a body comprising the blunted and the first conical segment only. This portion of the whole body is then regarded as the "bluntness" and steps 2) to 8) are repeated for a body consisting of this "bluntness" and the next conical segment. The shock wave due to the "isolated bluntness is, of course taken from the previous calculation as is the drag of the "bluntness". Repeated application of this procedure allows any number of additional conical segments to be treated.

5. Testing of accuracy of method

Any reasonably general prediction method may be tested in two ways:-

a) by comparison of predicted and experimental results for a multiplicity of cases covering the whole range of interest,

or b) by comparison of predicted and experimental values in selected cases chosen so as to test the main assumptions implicit in the calculation method.

The former procedure is extremely arduous and time consuming. The latter procedure is not only more convenient but it provides clearer indications of those areas in which improvements in the prediction method are most desirable. This method has, therefore, been adopted.

There are three main sets of approximations implicit in the method. These are:-

a) the method adopted to match the solutions for Zones I and II.

b) the representation of the effects of the entropy layer.

c) the approximations made in the calculation of Zone III.

The last set of approximations may be tested by computing the drag of a range of sharp cones. Clearly, in this case the first two sets of assumptions do not enter the calculation. As over 60% of the total drag is then associated with entropy production in Zone III, this is a severe test of the accuracy with which this region is calculated. The results of such calculations are shown in Fig. (3) where it will be seen that reasonable agreement exists between the predicted forebody pressure drags and the exact solutions available for this particular case. Significant discrepancies of absolute level are present at the lower fineness ratios. However, the curves are clearly of the same form and the effects of changes in fineness ratio are well predicted. Indeed, the derivative $\partial C_p/\partial(l/D)$ is predicted to an accuracy of better than 10% throughout the range shown. Fortunately, at the low fineness ratios, where the errors are greatest, the practical interest is least.

The first two sets of approximations cannot be tested completely independently of each other or of the last set. However the adequacy of both may be tested by calculating the forebody pressure drag of spherically blunted cones. Two series of calculations were performed. In the first of these, the variation of forebody drag with bluntness ratio for cones having a fixed semi-apex angle of 20° was computed. These results are compared with measurements made by Owen[6] and others, collated by the Royal Aeronautical Society[9] (Fig. (4)). The predictions are in reasonable agreement with the measured drags (and with the theoretical value for $(d/D)=0$). In the second series of calculations the bluntness ratio was varied while the fineness ratio was held constant at 2.0. These predictions were compared with the R. Ae. Soc. Data Sheets[9] (Fig. (5)). Again, reasonable agreement was obtained and it is gratifying to observe that occurrence of a drag minimum was correctly predicted and that the extent of the drag reduction effected by nose blunting and the optimum bluntness ratio is given approximately.

/An

An alternative presentation showing the accuracy of the method is given as Fig. (7). In this, the predicted drags of 22 sharp and spherically blunted cones are compared to values derived from R. Ae. S. Data Sheets[9]. The scatter of the predicted drags exceeds the quoted accuracy of the Data Sheets by less than ±5% for over 70% of the bodies considered.

It may be observed that good agreement is not confined to M = 3.05. Fig.(6) shows a comparison of predicted shock-wave shapes for a 40° semi-apex angle cone at M = 8.8 with measurements made in the NPL 16 in shock tunnel. The agreement is good and the slight divergence of measured and predicted shock-wave shapes with increasing distance downstream is consistent with the small gradient of freestream Mach number in the shock tunnel in which the measurements were made.[8]

Finally, the proposed method would become cumbersome if a large number of segments were needed to approximate a given, non-conical, body shape to sufficient accuracy. However, Fig. (8) shows the effect of varying the number of segments used to represent a tangent ogive. It will be seen that 8 segments are quite sufficient to give a reasonably accurate estimate of the drag.

6. Conclusions

A simple method for the prediction of forebody pressure drag has been developed. Although some refinement is needed the method appears to be promising. The novel feature of this method, which makes only limited use of empirical information, is that the drag is computed via the prediction of the shape of the complete bow shock wave. The development of this method has indicated the importance of the displacement effect of the entropy layer and has suggested a number of simplifying assumptions that may be of use in other applications. The method has already shown considerable promise for the prediction of the zero-lift drag of blunted axi-symmetric bodies, and future work will be concerned with the refinement of the method and its extension to include the lifting case and flow fields where strong internal shocks are present in the flow between the bow shock wave and the body. Such developments must, however, wait on further detailed experimental studies and since the method is currently capable of yielding useful results in cases of practical importance, it is felt that it is appropriate to present its basic elements at this stage.

7. Acknowledgements

The authors are anxious to acknowledge the assistance of many friends and colleagues. Noteable amongst these are Dr. A. Moore of R.A.E. and Mr. J. Arnall of H.S.A. (Kingston) who helped greatly in the provision of the characteristic solutions referred to in the text, Dr. R. C. Lock who contributed much valuable criticism and advice, and Dr. L. Davies, Mr. R. F. Cash, and Mr. A. Catley who obtained the M = 8.8 results, and Mr. J. Fulker (of N.P.L.) who performed much of the programming work.

Symbols

a	local speed of sound
A	maximum cross-sectional area of body
C_D	forebody pressure drag coefficient based on free-stream conditions and area A. $\left(C_D = \frac{K}{\frac{1}{2}\rho_\infty u_\infty^2 A} \right)$
C_p	pressure coefficient $\left(C_p = \frac{(p-p_\infty)}{\frac{1}{2}\rho_\infty u_\infty^2} \right)$
c_p	specific heat at constant pressure of air
c_v	specific heat at constant volume of air
d	diameter of body at bluntness/cone junction
D	base diameter of body
G	See text (equation (10))
ℓ	See text (Section 3.3)
L	length of body
K	total pressure drag of forebody
M	Mach number
p	static pressure
R	gas constant
ΔS	change in specific entropy of a given mass of air
S	total rate of entropy production
T	static temperature
u	velocity
y	distance from axis of symmetry measured perpendicular to free-stream direction
Z	See text (equation (6))
β	inclination of shock wave to free-stream direction
γ	adiabatic index $(\gamma = c_p/c_v)$
ξ	a small fraction change in drag (Section 3.2)

/η

η See Text (Section 3.2)

ϕ mean inclination of characteristic to free-stream direction

μ Mach angle = $\sin^{-1}(1/M_\infty)$

ϕ_s inclination of characteristic to free-stream direction immediately downstream of shock wave

ρ density

Suffices

∞ free-stream

d downstream of bow shock wave

s cone surface conditions.

References

No.	Author(s)	Title, etc.
1	K. Oswatitsch and G. Kuerti	Gas Dynamics Academic Press, 1956
2	P. G. Pugh and L. C. Ward	The Estimation of Zero Incidence Forebody Pressure Drag Coefficients of Axisymmetric Bodies from Measured Bow Shock Shapes. NPL Aero Report 1245, ARC 29 350, August, 1967.
3	J. L. Simms	Tables for Supersonic Flow Around Right Circular Cones at Zero Angle of Attack. NASA SP-3004 (1964)
4	R. S. Crabbe and G. S. Campbell	Tables of Derivatives to extend the zero incidence cone tables to intermediate Mach numbers and cone angles. N.R.C. 9136, May, 1966
5	A. Moore	Private Communication (RAE) 1968
6	R. V. Owens	Aerodynamics Characteristics of Spherically blunted cones at Mach Numbers from 0.5. to 5.0. NASA Tech. Note TN-D-3088, December, 1965
7	P. G. Pugh and M. J. Larcombe	A quantitative use of schlieren and shadowgraph systems. Visual, Vol. 7, No. 1 1969 (Pergamon Press)
8	L. Davies	Private Communication (NPL) 1969
9	Anon	Engineering Sciences Data Unit (Royal Aeronautical Society) Engineering Sciences Data Item 68021 (1968)
10	Anon	Engineering Sciences Data Unit (Royal Aeronautical Society) Engineering Sciences Data Item 502.03.03 (1954)
11	S. C. Traugott	Some features of supersonic and hypersonic flow about blunted cones. J. Aero Sci., Vol. 29, No. 4, April, 1962
12	R. W. Luidens	An estimate of the supersonic flow field about an axisymmetric body with an N-wave pressure trace. NASA TN D-4935, December, 1968.

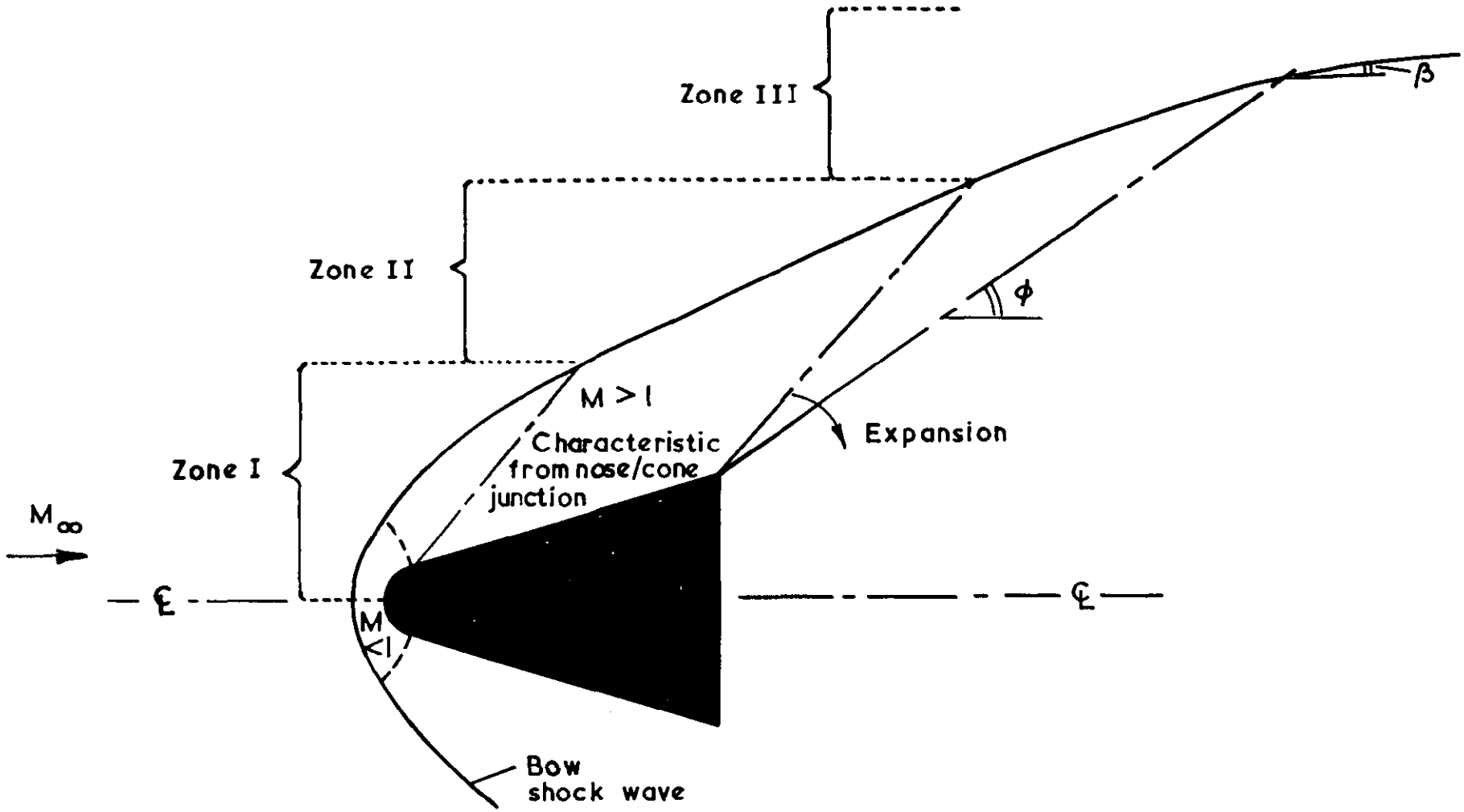

Schematic of flow over blunted body

FIG. 1

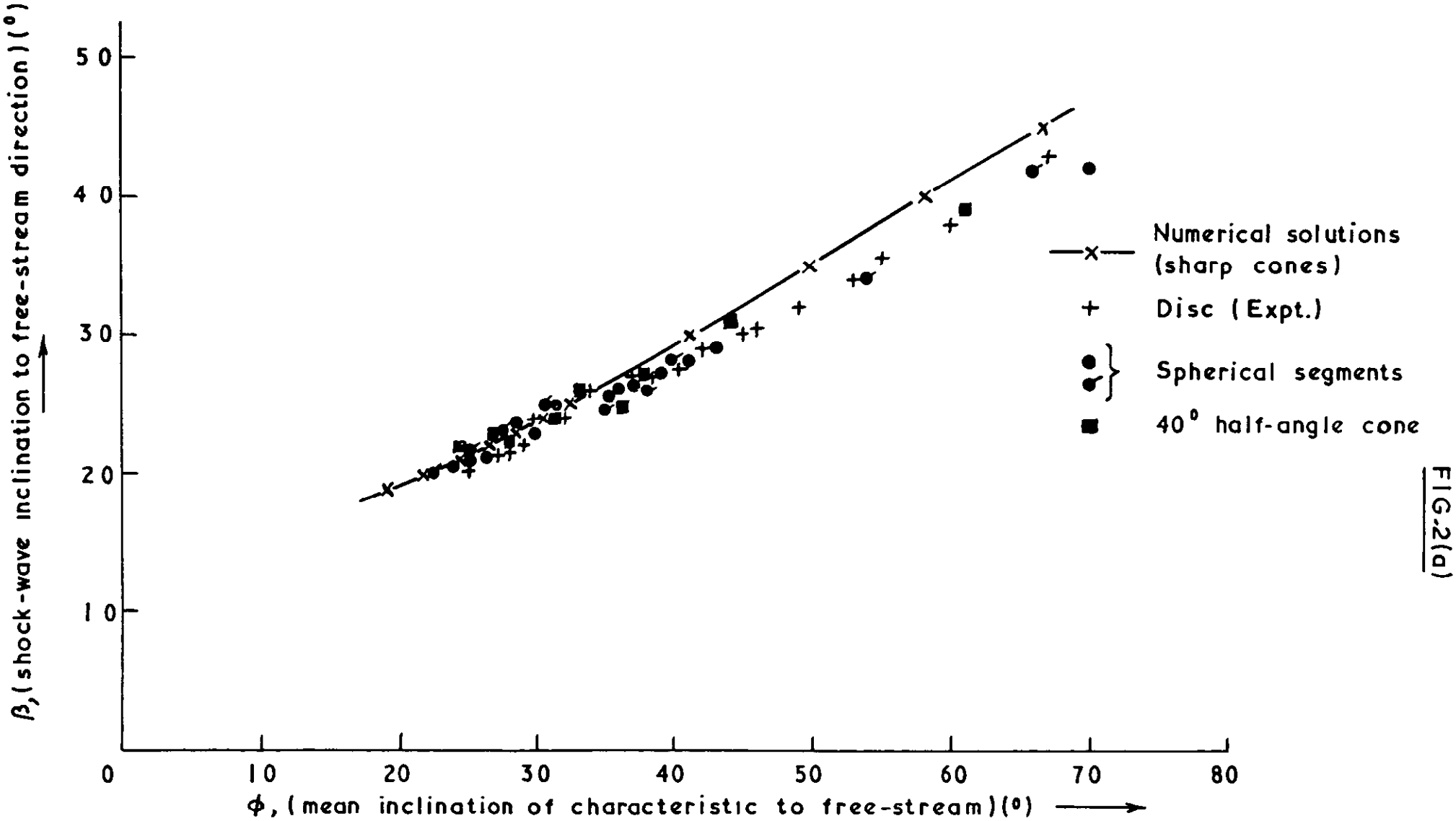

FIG.2(a)

M = 3·05

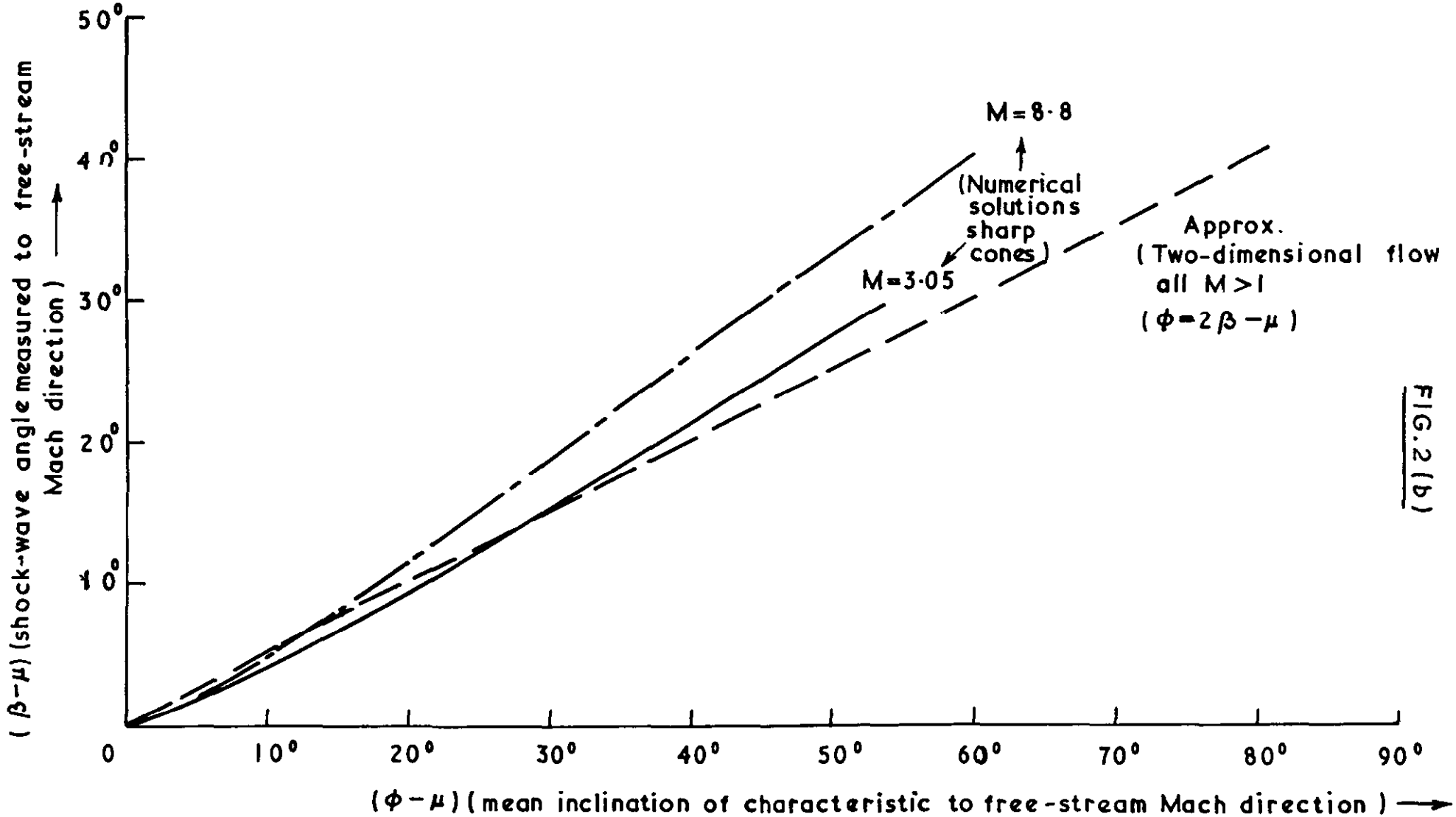

FIG. 2 (b)

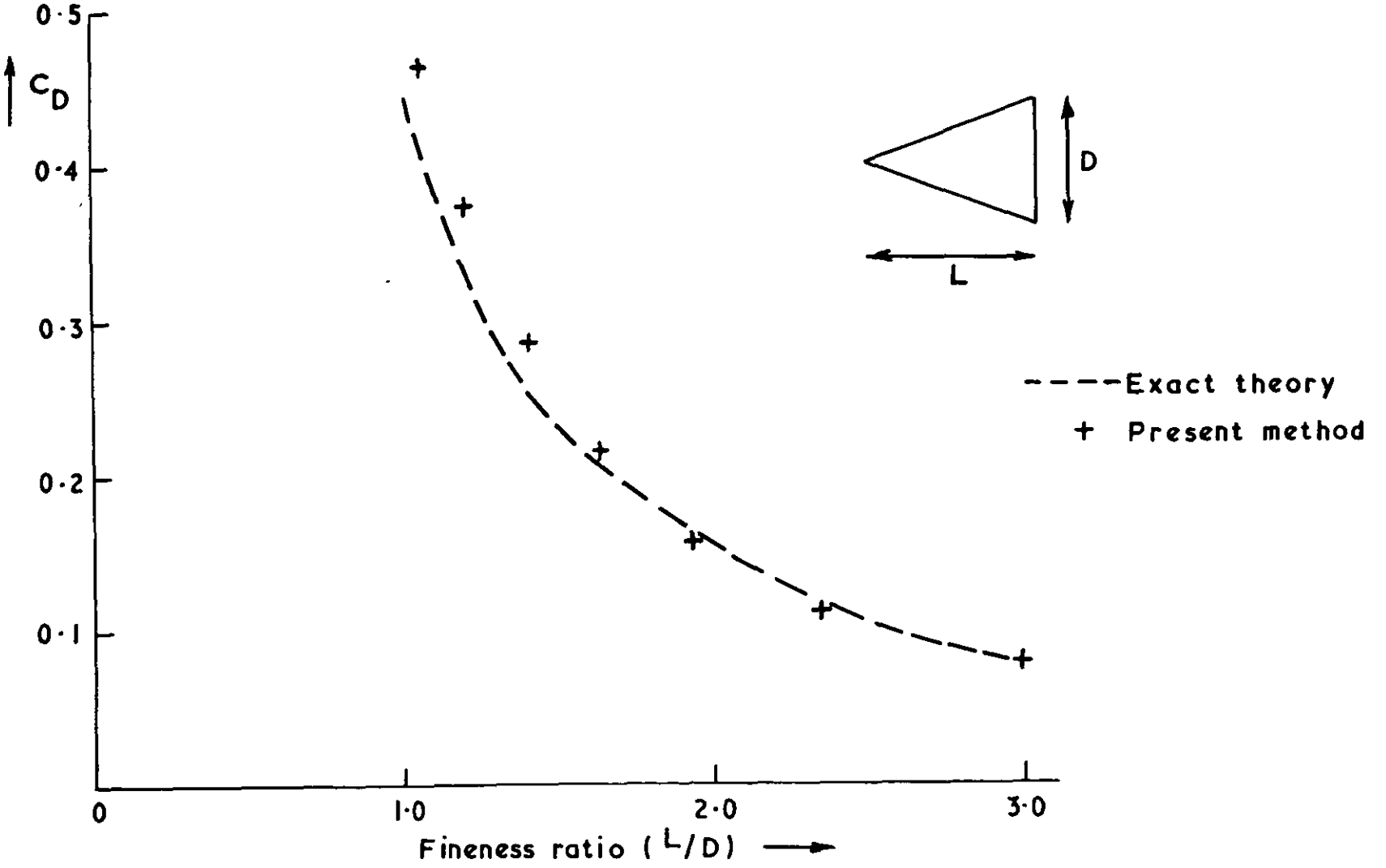

FIG.3

Sharp cones. M=3·05

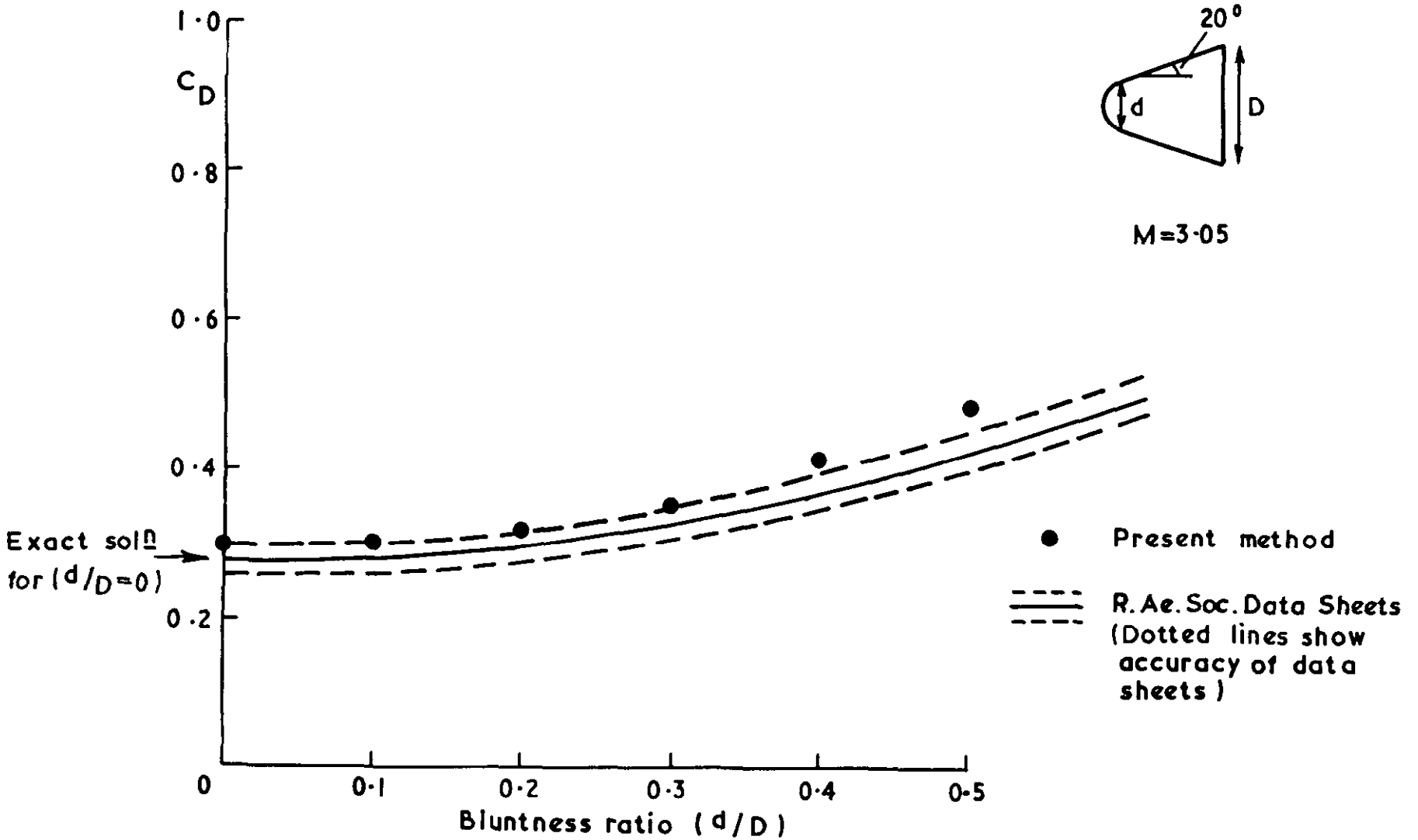

FIG. 4

Forebody drag of spherically blunted cones
(constant apex angle)

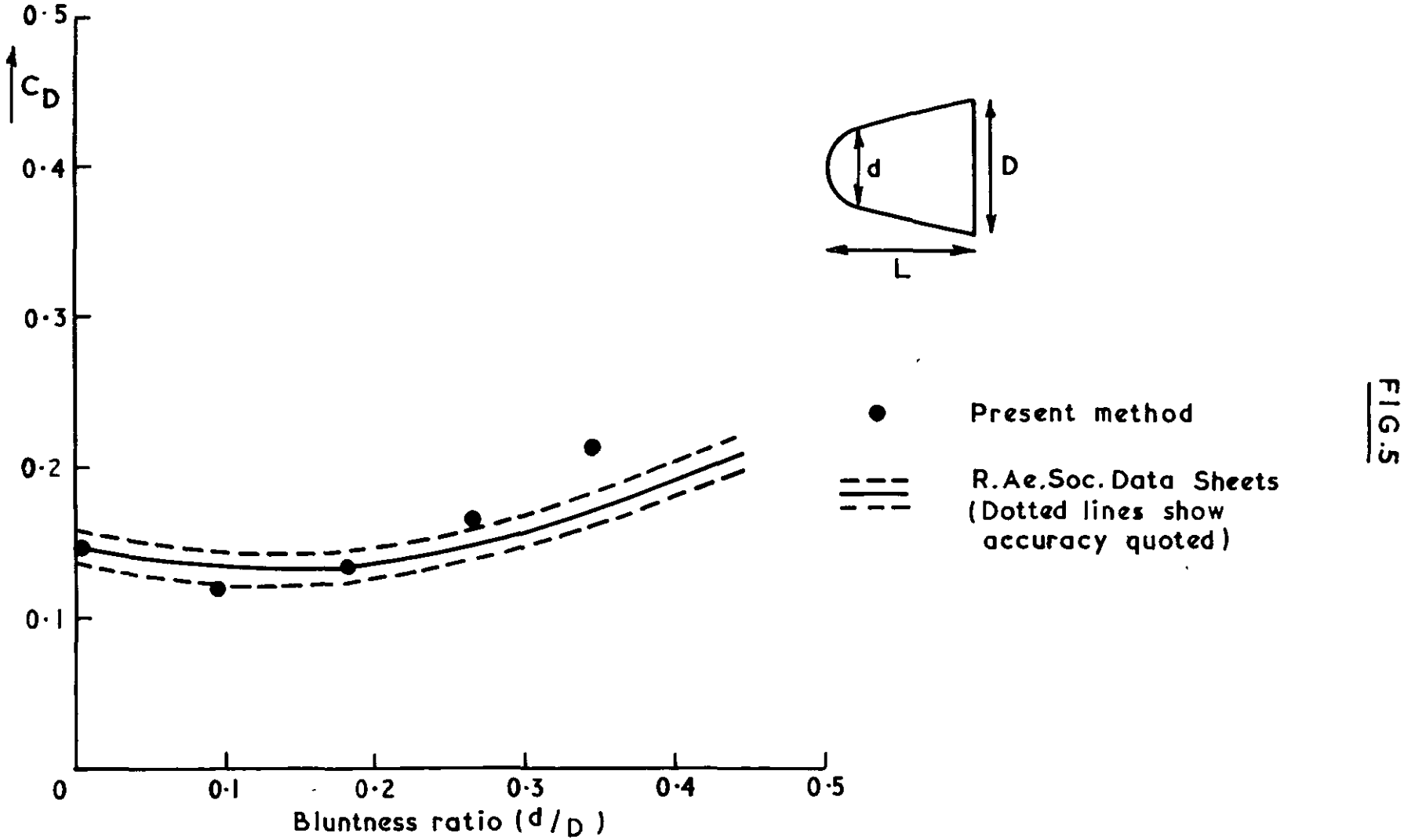

FIG.5

Blunt cones—constant fineness ratio (L/D) = 2 . M = 3·05

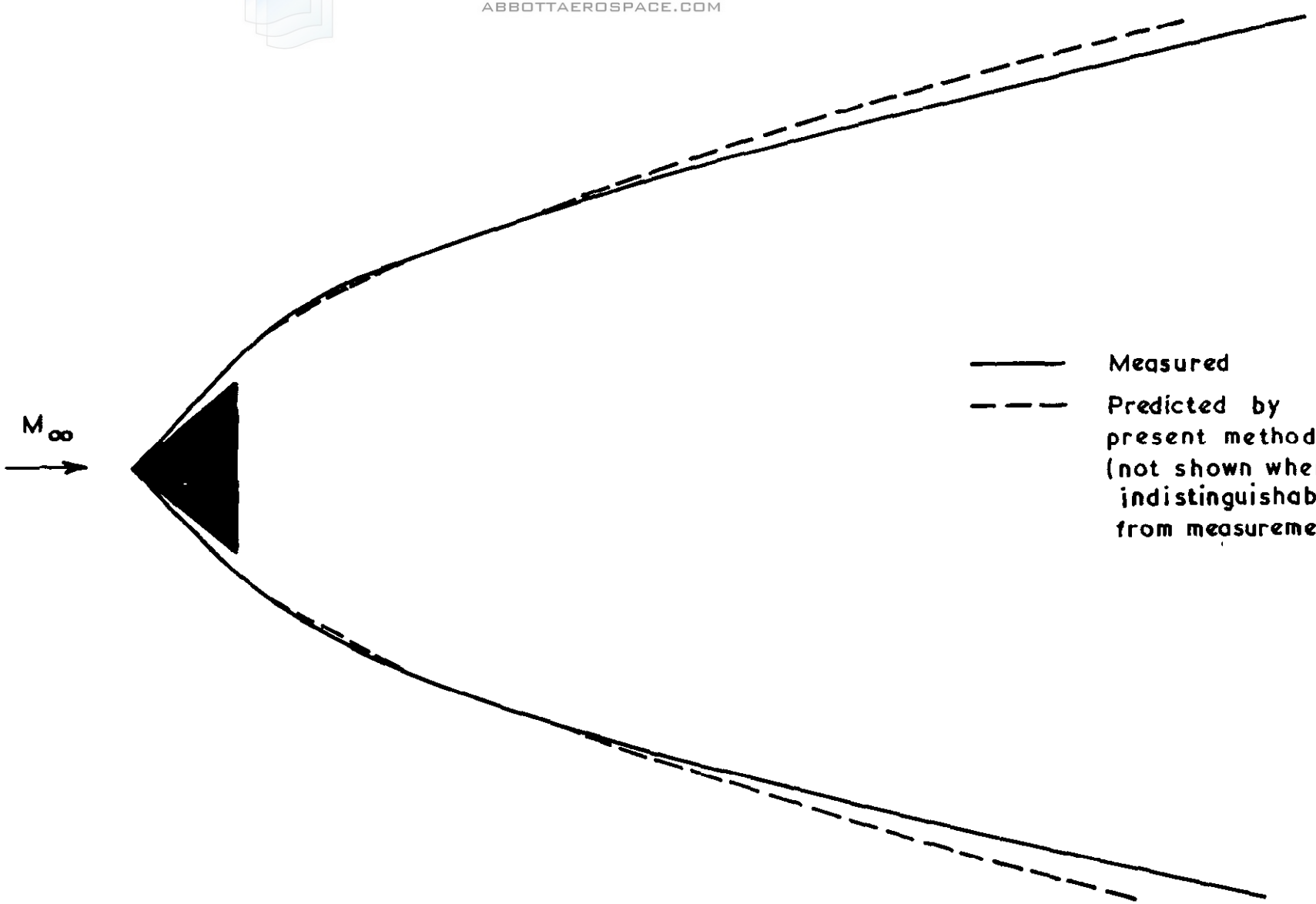

FIG.6

Bow shock-wave of a 40° half-angle cone

$M_\infty = 8 \cdot 8$

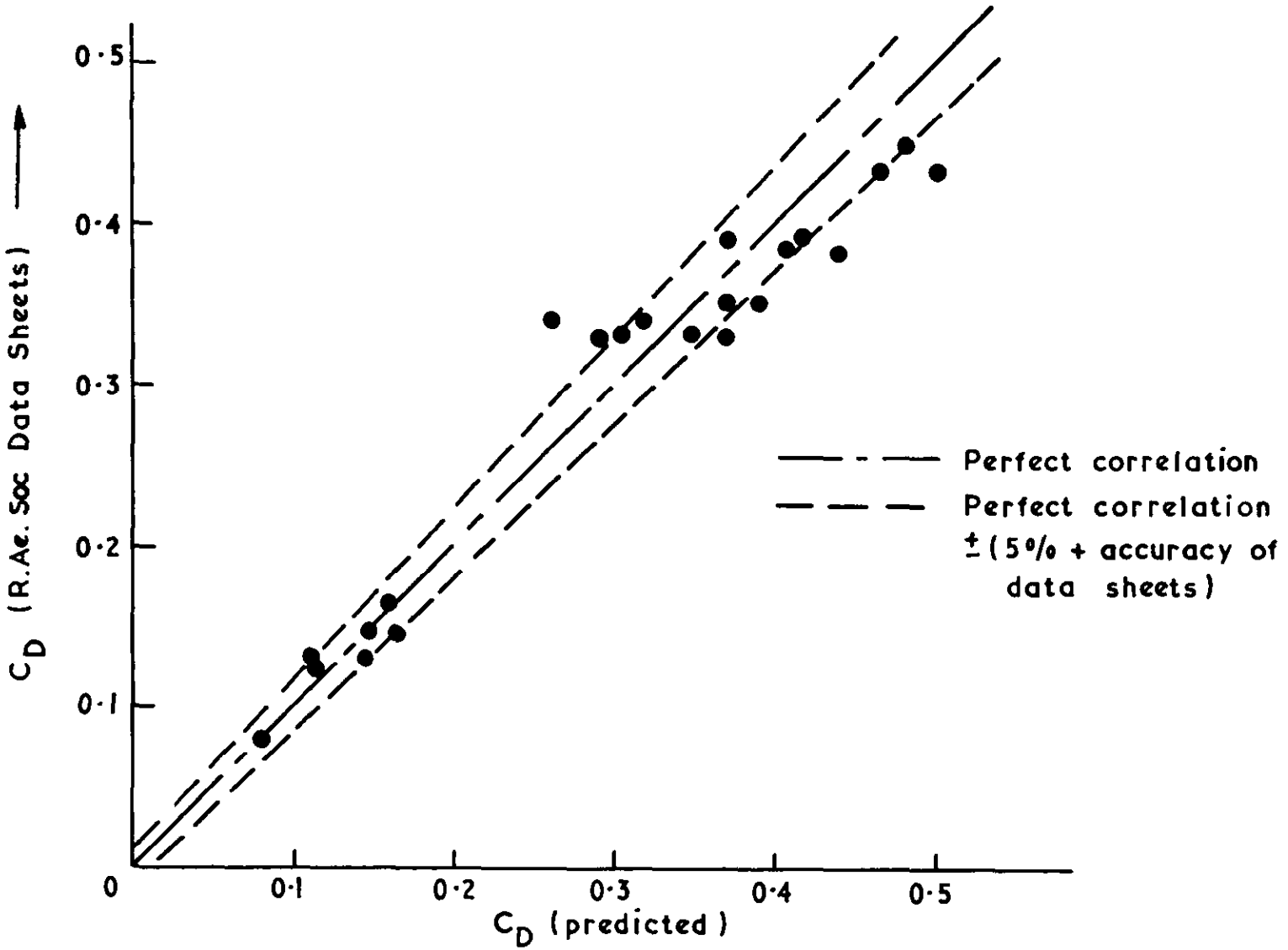

FIG.7

Correlation diagram for various spherically blunted cones. M=3·05

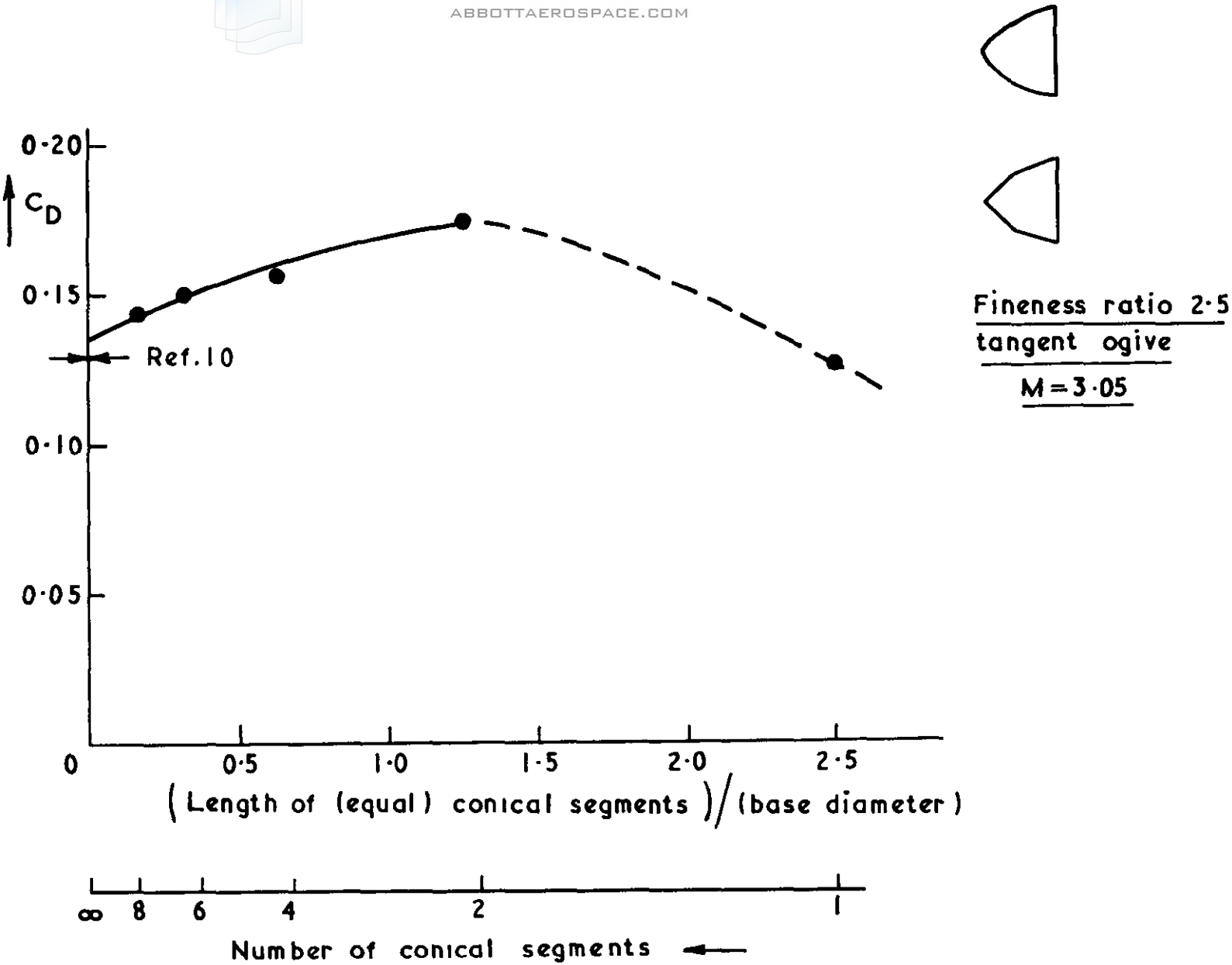

Fineness ratio 2·5
tangent ogive
M = 3·05

Effect of varying length of segments

FIG. 8

R129542/501371 K4 3/71 P

A.R.C. C.P. No.1142
February, 1970
Pugh, P. G. and Ward, L. C.

A NOVEL METHOD FOR THE ESTIMATION OF THE ZERO-LIFT FOREBODY PRESSURE DRAG OF AXISYMMETRIC NON-SLENDER SHAPES AT SUPERSONIC AND HYPERSONIC VELOCITIES

A method for calculating the zero-lift drag of both blunted and sharp forebodies is described. This uses the novel approach of first predicting the shape of the bow shock wave and then using this to compute the drag. Accuracies of drag prediction of typically 5% are achieved.

A.R.C. C.P. No.1142
February, 1970
Pugh, P. G. and Ward, L. C.

A NOVEL METHOD FOR THE ESTIMATION OF THE ZERO-LIFT FOREBODY PRESSURE DRAG OF AXISYMMETRIC NON-SLENDER SHAPES AT SUPERSONIC AND HYPERSONIC VELOCITIES

A method for calculating the zero-lift drag of both blunted and sharp forebodies is described. This uses the novel approach of first predicting the shape of the bow shock wave and then using this to compute the drag. Accuracies of drag prediction of typically 5% are achieved.

A.R.C. C.P. No.1142
February, 1970
Pugh, P. G. and Ward, L. C.

A NOVEL METHOD FOR THE ESTIMATION OF THE ZERO-LIFT FOREBODY PRESSURE DRAG OF AXISYMMETRIC NON-SLENDER SHAPES AT SUPERSONIC AND HYPERSONIC VELOCITIES

A method for calculating the zero-lift drag of both blunted and sharp forebodies is described. This uses the novel approach of first predicting the shape of the bow shock wave and then using this to compute the drag. Accuracies of drag prediction of typically 5% are achieved.

DETACHABLE ABSTRACT CARDS

Produced and published by
HER MAJESTY'S STATIONERY OFFICE

To be purchased from
49 High Holborn, London WC1V 6HB
13a Castle Street, Edinburgh EH2 3AR
109 St Mary Street, Cardiff CF1 1JW
Brazennose Street, Manchester M60 8AS
50 Fairfax Street, Bristol BS1 3DE
258 Broad Street, Birmingham B1 2HE
80 Chichester Street, Belfast BT1 4JY
or through booksellers

Printed in England

C.P. No. 1142

SBN 11 470390 6